Thermochimica Acta, 112 (1987) 275–287
Elsevier Science Publishers B.V., Amsterdam – Printed in The Netherlands

THERMAL DECOMPOSITION REACTIONS OF METAL CARBOXYLATO COMPLEXES IN THE SOLID STATE. II. THERMOGRAPHIC AND DIFFERENTIAL THERMAL STUDIES OF METAL OXALATO, MALONATO AND SUCCINATO COMPLEXES

H.L. SAHA and S. MITRA *

Department of Chemistry, Manipur University, Imphal 795 003 (India)

(Received 7 July 1986)

ABSTRACT

The thermal investigations of metal carboxylato complexes of the first transition metals, Mn(II), Fe(II), Fe(III), Co(II), Ni(II) and Cu(II) and non transition metals like Zn(II) and Cd(II) in solid state were carried out under non-isothermal condition in nitrogen atmopshere by thermogravimetric (TG) and differential thermal analyses (DTA) methods. The results of DTA curves inferred that the thermal stability of the complex decreased approximately with the increase of standard potential of the central metal ion. The thermal parameters like activation energy (E_a^*), enthalpy change (ΔH) and entropy change (ΔS) corresponding to deaquation, deammoniation and decomposition processes occurred simultaneously or separately were determined from TG and DTA curves by the standard methods. A linear correlation has been found in the plots of ΔH vs. ΔS and E_a^* vs. ΔS in deaquation, deammoniation and decomposition processes. An irreversible phase transition was noticed for $H_2[Mn(suc)_2]$ and $H_2[Co(suc)_2]$ complexes in DTA curves. The residual pyrolysed products were metal carbonates.

INTRODUCTION

Thermal investigations of transition metal oxalato, malonato and succinato complexes having ammonium ion (NH_4^+) outside the coordination sphere has been carried out. Complexes were prepared of the type: $(NH_4)_2[ML_2] \cdot nH_2O$ and $(NH_4)_3[FeL_3] \cdot nH_2O$, where, M = Mn(II), Fe(II), Co(II), Ni(II), Cu(II), Zn(II) and Cd(II); L = oxalate, malonate and succinate ligands and $n = 1$ to 7. The present paper reports the characterization of the complexes by elemental analyses and the thermal investigations under non-isothermal condition. The conversion of $[FeL_3]^{3-} \rightarrow [FeL_2]^{2-}$ was initiated by electron transfer from the coordinated ligand ion to the central metal ion [1]. The thermodynamic parameters like activation energy (E_a^*), enthalpy change (ΔH) and entropy change (ΔS) have been discussed and some useful conclusions were drawn.

0040-6031/87/$03.50

EXPERIMENTAL

The complexes of the type, $(NH_4)_2[ML_2] \cdot nH_2O$ and $(NH_4)_3[FeL_3] \cdot nH_2O$ were synthesised by the following general methods (for Fe^{3+} complex the ratio of metal salt to ligand is 1 : 3). The hydrated metal halide (2.0 mmol) in distilled water (10 ml) was mixed with a solution of the ligand (4.0 mmol) in same solvent (10 ml) and the mixture stirred for 0.5 h to precipitate the complex. The product was collected, washed with water and ethanol and dried in a desiccator (yield 60–65%). The chemicals used were Analar grade B.D.H. products. Certain modifications have been made in case of malonato complexes due to their higher solubilities in aqueous medium. The complexes were characterized by elemental analyses with standard semimicro techniques (Table 1).

Thermal decompositions were carried out in a constant flow of nitrogen with platinum crucible using α-Al_2O_3 as standard. Thermogravimetric analysis (TG) and differential thermal analysis (DTA) curves were recorded simultaneously by DT-30 thermal analyser (Shimadzu, Japan) keeping the heating rate at $10°C\ min^{-1}$ for each run using 10–20 mg dry powdered sample. The enthalpy changes (ΔH) were calculated from the DTA peak area using indium metal as standard and their corresponding entropy changes (ΔS) were also calculated. Infrared spectra were recorded with a Perkin Elmer 783 IR spectrometer in KBr medium.

RESULTS AND DISCUSSION

The TG and DTA curves of some metal oxalato, malonato and succinato complexes are shown in Figs. 1, 2 and 3, respectively. The oxalato complexes of Co(II) and Zn(II) are monohydrate, Ni(II) is trihydrate and the rest are dihydrates. For malonato complexes, Mn(II) and Zn(II) are monohydrates, Fe(II) and Co(II) are trihydrate and heptahydrate respectively, the rest are dihydrates. In the succinato series, the Fe(III) and Zn(II) complexes are anhydrous while the Cd(II) complex is dihydrate, and the Fe(II), Co(II) and Cu(II) complexes are trihydrates. Mn(II) and Ni(II) complexes are tetrahydrates. In oxalato series, the deaquation and deammoniation occurred in a single step for the Mn(II), Co(II), Zn(II) and Cd(II) complexes. For the Fe(III), Ni(II) and Cu(II) complexes, the deaquation occurred in the first step followed by deammoniation which were confirmed by ammonia test. The conversion of $(NH_4)_2[Fe(ox)_2] \cdot 2H_2O \rightarrow FeCO_3$ occurred in a single step as shown in Table 2. For malonato complexes, deaquation and deammoniation occurred in a single step except, $(NH_4)_3[Fe(mal)_3] \cdot 2H_2O$, where deaquation was followed by deammoniation (Table 3).

In the succinato series all the complexes lost their water and ammonia molecules in a single step, except $(NH_4)_2[Cu(suc)_2] \cdot 3H_2O$, where deaqua-

TABLE 1

Analytical data of metal oxalato (ox), malonato (mal) and succinato (suc) complexes

Compound	Elemental analyses (%) [a]		Compound	Elemental analyses (%) [a]		Compound	Elemental analyses (%) [a]	
	Central metal	Carbon		Central metal	Carbon		Central metal	Carbon
$(NH_4)_2[Mn(ox)_2]\cdot 2H_2O$	17.92(18.14)	15.31(15.84)	$(NH_4)_2[Mn(mal)_2]\cdot H_2O$	17.32(17.56)	22.88(23.00)	$(NH_4)_2[Mn(suc)_2]\cdot 4H_2O$	13.58(13.91)	24.00(24.30)
$(NH_4)_2[Fe(ox)_2]\cdot 2H_2O$	18.08(18.38)	15.20(15.80)	$(NH_4)_2[Fe(mal)_2]\cdot 3H_2O$	15.36(15.96)	20.60(20.58)	$(NH_4)_2[Fe(suc)_2]\cdot 3H_2O$	14.38(14.78)	25.92(25.40)
$(NH_4)_3[Fe(ox)_3]\cdot 2H_2O$	13.72(13.62)	17.00(17.56)	$(NH_4)_3[Fe(mal)_3]\cdot 2H_2O$	12.30(12.36)	23.13(23.90)	$(NH_4)_3[Fe(suc)_3]$	12.00(12.20)	31.11(31.45)
$(NH_4)_2[Co(ox)_2]\cdot H_2O$	20.11(20.39)	16.80(16.61)	$(NH_4)_2[Co(mal)_2]\cdot 7H_2O$	13.95(13.87)	17.01(16.94)	$(NH_4)_2[Co(suc)_2]\cdot 3H_2O$	15.28(15.47)	25.84(25.20)
$(NH_4)_2[Ni(ox)_2]\cdot 3H_2O$	17.66(18.08)	14.05(14.78)	$(NH_4)_2[Ni(mal)_2]\cdot 2H_2O$	17.90(17.54)	21.98(21.51)	$(NH_4)_2[Ni(suc)_2]\cdot 4H_2O$	14.88(14.72)	24.88(24.08)
$(NH_4)_2[Cu(ox)_2]\cdot 2H_2O$	20.99(20.38)	15.66(15.40)	$(NH_4)_2[Cu(mal)_2]\cdot 2H_2O$	18.48(18.70)	21.10(21.20)	$(NH_4)_2[Cu(suc)_2]\cdot 3H_2O$	16.61(16.47)	24.21(24.90)
$(NH_4)_2[Zn(ox)_2]\cdot H_2O$	22.88(22.13)	16.11(16.25)	$(NH_4)_2[Zn(mal)_2]\cdot H_2O$	20.08(20.22)	22.19(22.26)	$(NH_4)_2[Zn(suc)_2]$	19.41(19.61)	28.23(28.79)
$(NH_4)_2[Cd(ox)_2]\cdot 2H_2O$	31.00(31.18)	13.00(13.32)	$(NH_4)_2[Cd(mal)_2]\cdot 2H_2O$	28.91(28.94)	18.09(18.54)	$(NH_4)_2[Cd(suc)_2]\cdot 2H_2O$	26.77(26.99)	22.69(23.05)

[a] Figures in parentheses are the calculated values

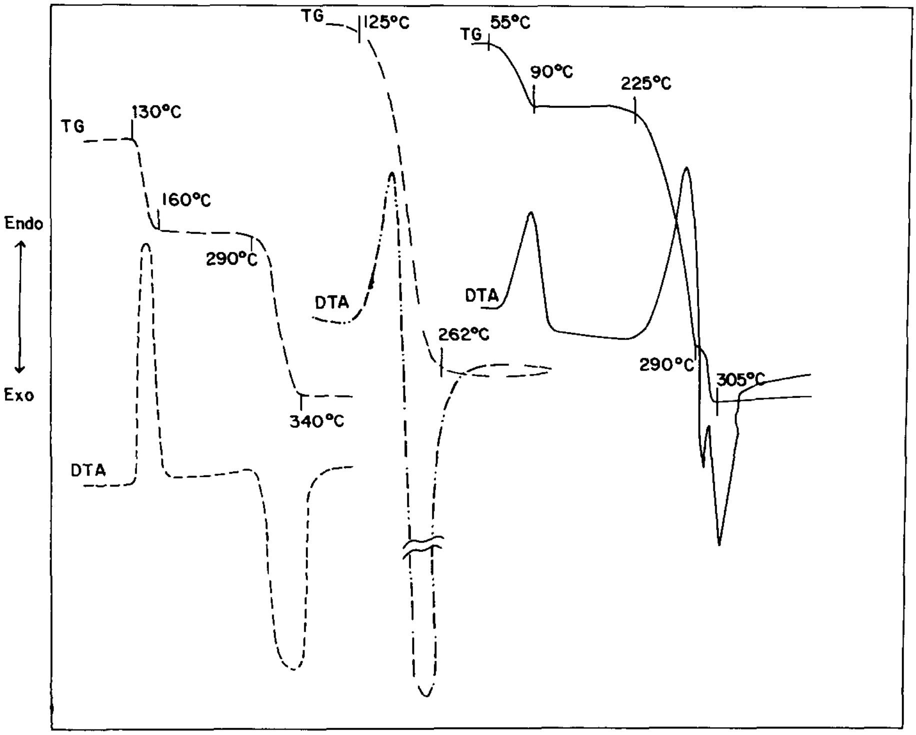

Fig. 1. Thermal curves of: (------) $(NH_4)_2[Mn(ox)_2]\cdot 2H_2O$, sample mass 10.6 mg; (-··-···) $(NH_4)_2[Fe(ox)_2]\cdot 2H_2O$, sample mass 14.72 mg; (———) $(NH_4)_2[Cu(ox)_2]\cdot 2H_2O$, sample mass 14.07 mg.

tion preceeds deammoniation. Fe(III) and Zn(II) complexes have no lattice water and they are converted to $FeCO_3$ and $ZnCO_3$ in multiple steps and a single step, respectively.

Temperature ranges of deaquation and deammoniation processes (occurring simultaneously or separately) are 30–338°C, 45–260°C and 30–168°C for oxalato, malonato and succinato complexes as shown in Tables 2, 3 and 4, respectively.

The TG and DTA curves of oxalato complexes show a single step decomposition, except, $(NH_4)_2[Cu(ox)_2]$, which decomposes through an unstable intermediate $H_2[Cu_2(Ox)_2]$, where copper is expected in univalent state (Table 2). A single step decomposition was observed for the conversion of $(NH_4)_2[Fe(ox)_2]\cdot 2H_2O \rightarrow FeCO_3$ in the TG curve but in the DTA curve two peaks were noticed at 205°C and 230°C as shown in Table 2 and Fig. 1. The TG curves for all the malonato complexes show a single step decomposition except for the Fe(II) and Fe(III) complexes. In the Fe(II) complex the decomposition proceeds via an unstable intermediate $H_2[Fe(mal)]$. For the Fe(III) complex the intermediate steps involve the

TABLE 2

Dehydration and decomposition reactions of metal oxalato complexes

Decomposition reactions	Temperature range (°C)	DTA peak temperature (°C)		Activation energy (E_a^*) (kJ mol^{-1})		ΔH (kJ mol^{-1})	ΔS (J K^{-1} mol^{-1})
		Endo	Exo	TG	DTA		
1 $(NH_4)_2[Mn(C_2O_4)_2]\cdot 2H_2O \rightarrow H_2[Mn(C_2O_4)_2]$	130–160	145		111.3	128.9	178.0	425.8
$H_2[Mn(C_2O_4)_2] \rightarrow MnCO_3$	290–340		325	205.0	231.8	197.0	329.6
2 $(NH_4)_2[Fe(C_2O_4)_2]\cdot 2H_2O \rightarrow FeCO_3$	125–262	205	230	100.0	109.2 [a], 96.6 [b]	95.6 [a], 213.8 [b]	200.0 [a], 425.0 [b]
3 $(NH_4)_3[Fe(C_2O_4)_3]\cdot 2H_2O \rightarrow (NH_4)_3[Fe(C_2O_4)_3]$	30–95	90		52.5	42.8	55.5	152.8
$(NH_4)_3[Fe(C_2O_4)_3] \rightarrow FeCO_3$	185–250		230	264.2	193.2	159.1	316.3
4 $(NH_4)_2[Co(C_2O_4)_2]\cdot H_2O \rightarrow H_2[Co(C_2O_4)_2]$	145–200	185		125.0	126.5	125.0	272.2
$H_2[Co(C_2O_4)_2] \rightarrow CoCO_3$	295–340		320	220.0	296.1	183.8	309.9
5 $(NH_4)_2[Ni(C_2O_4)_2]\cdot 3H_2O \rightarrow (NH_4)_2[Ni(C_2O_4)_2]$	180–262	250		103.4	122.7	117.2	224.1
$(NH_4)_2[Ni(C_2O_4)_2] \rightarrow H_2[Ni(C_2O_4)_2]$	262–338		335	86.6	–	123.0 [c]	–
$H_2[Ni(C_2O_4)_2] \rightarrow NiCO_3$	338–375		370	300.0	–		–
6 $2(NH_4)_2[Cu(C_2O_4)_2]\cdot 2H_2O \rightarrow 2(NH_4)_2[Cu(C_2O_4)_2]$	55– 90	80		197.4	193.2	70.5	199.6
$2(NH_4)_2[Cu(C_2O_4)_2] \rightarrow H_2[Cu_2(C_2O_4)_2]$	225–290	275		139.0	128.8	170.0	301.9
$H_2[Cu_2(C_2O_4)_2] \rightarrow 2CuCO_3$	290–305		290	–	–	–	–
7 $(NH_4)_2[Zn(C_2O_4)_2]\cdot H_2O \rightarrow H_2[Zn(C_2O_4)_2]$	125–175	165		100.0	90.3	75.0	171.2
$H_2[Zn(C_2O_4)_2] \rightarrow ZnCO_3$	355–400		385	430.0	338.1	48.9	73.2
8 $(NH_4)_2[Cd(C_2O_4)_2]\cdot 2H_2O \rightarrow H_2[Cd(C_2O_4)_2]$	70–130	115		76.3	79.9	167.3	431.2
$H_2[Cd(C_2O_4)_2] \rightarrow CdCO_3$	310–355		340	370.0	323.4	79.3	130.4

[a] For deaquation and deammoniation.

[b] For decarboxylation.

[c] Overall enthalpy change for deammoniation and decarboxylation.

TABLE 3

Dehydration and decomposition reactions of metal malonato complexes

Decomposition reactions	Temperature range (°C)	DTA peak temperature (°C)		Activation energy (E_a^*) (kJ mol^{-1})		ΔH (kJ mol^{-1})	ΔS (J K^{-1} mol^{-1})
		Endo	Exo	TG	DTA		
1 $(NH_4)_2[Mn(C_3H_2O_4)_2]\cdot H_2O \rightarrow H_2[Mn(C_3H_2O_4)]$	50–190	82, 120, 175		44.8	–	96.7	–
$H_2[Mn(C_3H_2O_4)] \rightarrow MnCO_3$	190–315	245, 285		60.7	–	96.8	–
2 $(NH_4)_2[Fe(C_3H_2O_4)_2]\cdot 3H_2O \rightarrow H_2[Fe(C_3H_2O_4)_2]$	55–145	115		72.3	96.6	200.7	517.3
$H_2[Fe(C_3H_2O_4)_2] \rightarrow H_2[Fe(C_3H_2O_4)]$	145–280		210, 250, 275	58.7	–	158.3 [a]	–
$H_2[Fe(C_3H_2O_4)] \rightarrow FeCO_3$	280–420		295, 350	33.0	–		–
3 $(NH_4)_3[Fe(C_3H_2O_4)_3]\cdot 2H_2O \rightarrow (NH_4)_3[Fe(C_3H_2O_4)_3]$	45–150	62		29.7	–	109.8	–
$(NH_4)_3[Fe(C_3H_2O_4)_3] \rightarrow H_2[Fe(C_3H_2O_4)_2]$	150–250	205	240	85.9	–		–
$H_2[Fe(C_3H_2O_4)_2] \rightarrow FeCO_3$	250–330		– [b]	91.9	–	123.8	–
4 $(NH_4)_2[Co(C_3H_2O_4)_2]\cdot 7H_2O \rightarrow H_2[Co(C_3H_2O_4)_2]$	110–190	140		61.6	50.2	181.3	439.0
$H_2[Co(C_3H_2O_4)_2] \rightarrow CoCO_3$	265–305		295	199.5		197.0	346.9
5 $(NH_4)_2[Ni(C_3H_2O_4)_2]\cdot 2H_2O \rightarrow H_2[Ni(C_3H_2O_4)_2]$	185–260	240		141.0	150.9	131.8	256.9
$H_2[Ni(C_3H_2O_4)_2] \rightarrow NiCO_3$	322–385		338, 346, 378	237.9	–	269.2	–
6 $(NH_4)_2[Cu(C_3H_2O_4)_2]\cdot 2H_2O \rightarrow H_2[Cu(C_3H_2O_4)_2]$	60–155	140		68.0	135.0	124.8	302.2
$H_2[Cu(C_3H_2O_4)_2] \rightarrow CuCO_3$	240–255		250	–	–	–	–
7 $(NH_4)_2[Zn(C_3H_2O_4)_2]\cdot H_2O \rightarrow H_2[Zn(C_3H_2O_4)_2]$	90–160	150		85.4	89.2	81.4	192.5
$H_2[Zn(C_3H_2O_4)_2] \rightarrow ZnCO_3$	270–318	285	310, 315	130.3	–	–	–
8 $(NH_4)_2[Cd(C_3H_2O_4)_2]\cdot 2H_2O \rightarrow H_2[Cd(C_3H_2O_4)]$	120–205	170, 195		77.8	–	65.4	–
$H_2[Cd(C_3H_2O_4)] \rightarrow CdCO_3$	225–275	240, 250		312.5	–	50.1	–

[a] Overall enthalpy change.

[b] No sharp peak obtained.

TABLE 4

Dehydration and decomposition reactions of metal succinato complexes

Decomposition reactions	Temperature range (°C)	DTA peak temperature (°C)		Activation energy (E_a^*) (kJ mol^{-1})		ΔH (kJ mol^{-1})	ΔS (J K^{-1} mol^{-1})
		Endo	Exo	TG	DTA		
1 $(NH_4)_2[Mn(C_4H_4O_4)_2]\cdot 4H_2O \rightarrow H_2[Mn(C_4H_4O_4)_2]$	70–150	110		107.1	88.6	259.7	672.9
$H_2[Mn(C_4H_4O_4)_2] \xrightarrow[\text{change}]{\text{Phase}} H_2[Mn(C_4H_4O_4)_2]$	240–315		270, 300	–	–	41.1	–
$H_2[Mn(C_4H_4O_4)_2] \rightarrow MnCO_3$	320–460		395	68.9	–	79.9	119.6
2 $(NH_4)_2[Fe(C_4H_4O_4)_2]\cdot 3H_2O \rightarrow H_2[Fe(C_4H_4O_4)_2]$	62–142	120		73.9	77.3	60.7	154.6
$H_2[Fe(C_4H_4O_4)_2] \rightarrow FeCO_3$	275–385		335	100.8	96.6	326.3	545.6
3 $(NH_4)_3[Fe(C_4H_4O_4)_3] \rightarrow H_3[Fe(C_4H_4O_4)_3]$	30–150	95		36.1	– [a]	18.5	50.2
$H_3[Fe(C_4H_4O_4)_3] \rightarrow H_2[Fe(C_4H_4O_4)2\frac{1}{2}]$	150–265		260	32.6	–	–	–
$H_2[Fe(C_4H_4O_4)2\frac{1}{2}] \rightarrow H_2[Fe(C_4H_4O_4)_2]$	265–300		280	–	–	–	–
$H_2[Fe(C_4H_4O_4)_2] \rightarrow FeCO_3$	300–475		400	85.7	60.9	322.4	479.0
4 $(NH_4)_2[Co(C_4H_4O_4)_2]\cdot 3H_2O \rightarrow H_2[Co(C_4H_4O_4)_2]$	80–155	130		75.4	64.3	248.1	615.5
$H_2[Co(C_4H_4O_4)_2] \xrightarrow[\text{change}]{\text{Phase}} H_2[Co(C_4H_4O_4)_2]$	245–280		278	–	–	18.9	34.3
$H_2[Co(C_4H_4O_4)_2] \rightarrow CoCO_3$	355–460		395, 440	47.0	–	383.9	–
5 $(NH_4)_2[Ni(C_4H_4O_4)_2]\cdot 4H_2O \rightarrow H_2[Ni(C_4H_4O_4)_2]$	100–168	140		86.7	67.2	252.4	611.1
$H_2[Ni(C_4H_4O_4)_2] \rightarrow NiCO_3$	365–405		380, 395	338.5	–	784.2	–
6 $(NH_4)_2[Cu(C_4H_4O_4)_2]\cdot 3H_2O \rightarrow (NH_4)_2[Cu(C_4H_4O_4)_2]$	45–100	85		68.0	69.3	124.4	342.7
$(NH_4)_2[Cu(C_4H_4O_4)_2] \rightarrow CuCO_3$	300–380		315, 340, 365	139.4	–	477.6	–
7 $(NH_4)_2[Zn(C_4H_4O_4)_2] \rightarrow ZnCO_3$	420–490		450	322.8	347.8	127.5	181.4
8 $(NH_4)_2[Cd(C_4H_4O_4)_2]\cdot 2H_2O \rightarrow H_2[Cd(C_4H_4O_4)]$	130–235	138, 218		72.8	–	140.5	–
$H_2[Cd(C_4H_4O_4)] \rightarrow H_2[Cd(C_4H_4O_4)_{1/2}]$	235–300	280		–	–	36.9	66.6
$H_2[Cd(C_4H_4O_4)_{1/2}] \rightarrow CdCO_3$	365–425		380	–	251.2	110.1	168.5

[a] Poor resolution of DTA peak.

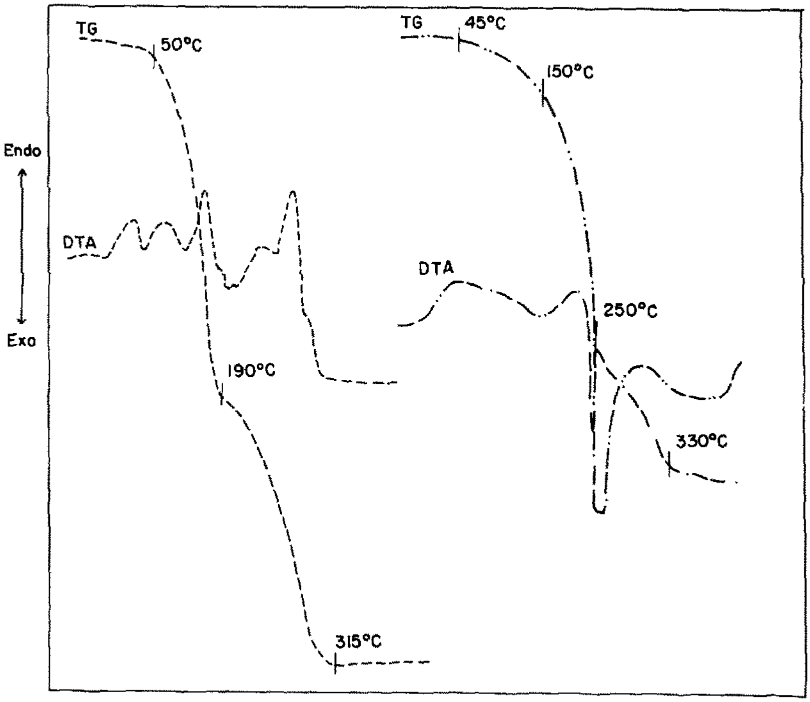

Fig. 2. Thermal curves of: (- - - - -) $(NH_4)_2[Mn(mal)_2]\cdot H_2O$, sample mass 19.8 mg; (-·-·-·-·) $(NH_4)_3[Fe(mal)_3]\cdot 2H_2O$, sample mass 13.7 mg.

conversion of $(NH_4)_3[Fe(mal)_3] \rightarrow H_2[Fe(mal)_2]$ showing two peaks in the DTA curve followed by a single step decarboxylation forming the product $FeCO_3$ as shown in Table 3 (Fig. 2). Single step decarboxylation was observed for the Co(II) and Cu(II) complexes in their DTA curves. The two-step decomposition of the Mn(II) and Cd(II) complexes was confirmed by two endothermic peaks in each case. The DTA curve showed multiple peaks for the decomposition of Fe(II) and Ni(II) complexes, whereas for the Zn(II) complex two exothermic peaks were found (Table 3).

The TG curves for most of the succinato complexes involve a single step decomposition except for $H_3[Fe(suc)_3]$ and $H_2[Cd(suc)_2]$ where three- and two-step decompositions were observed as shown in Table 4. The reduction step of $Fe^{3+} \rightarrow Fe^{2+}$ is a two step process manifesting two exothermic peaks at 260°C and 280°C. The decomposition of $H_2[Cd(suc)] \rightarrow CdCO_3$ occurred in two steps via the intermediate $H_2[Cd(suc)_{1/2}]$ as observed by weight loss in the TG curve. The DTA curve also showed two peaks at 280°C (endo) and 380°C (exo). This type of observation was not noticed for oxalato and malonato complexes of Cd(II). The deammoniation and decomposition of $(NH_4)_2[Zn(suc)_2]$ occurred in a single step (Fig. 3). Such phenomena were

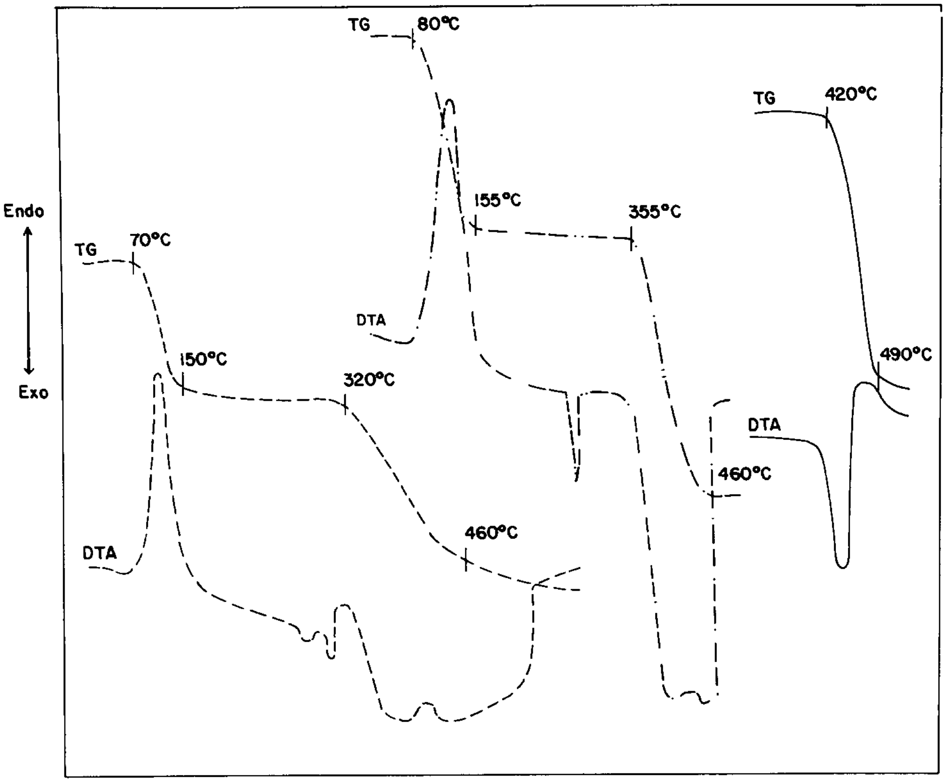

Fig. 3. Thermal curves of: (- - - - -) $(NH_4)_2[Mn(suc)_2]\cdot 4H_2O$, sample mass 11.17 mg; (- ·· - ·· -) $(NH_4)_2[Co(suc)_2]\cdot 3H_2O$, sample mass 16.0 mg; (———) $(NH_4)_2[Zn(suc)_2]$, sample mass 12.10 mg.

not observed in the case of oxalato and malonato complexes. Prominent phase transitions were noticed in DTA curves in the temperature ranges 240–315°C and 245–280°C for $H_2[Mn(suc)_2]$ and $H_2[Co(suc)_2]$ as shown in Table 4 and Fig. 3, while in the TG curves no weight loss was seen. In $H_2[Mn(suc)_2]$ two exothermic peaks appeared at 270°C and 300°C in the DTA curve, the first one being accompanied by a larger area compared to the second peak. A sharp exothermic peak was found for $H_2[Co(suc)_2]$ at 278°C.

The decomposition of Fe(III) complexes to $FeCO_3$ for oxalato, malonato and succinato complexes was observed in one, two and three steps, respectively, indicating the decreasing tendency of the electron transfer from the coordinate ligand ion to the central metal ion. This phenomenon is also supported by their decreasing order of DTA peak temperatures as ox < mal < suc (Tables 2–4).

In malonato and succinato complexes where deaquation and decomposition occurred in a single step, the DTA peak temperatures follow the trend: Ni(II) > Cd(II) > Zn(II) * > Co(II) ~ Cu(II) * > Fe(II) > Mn(II).

For the oxalato series, the order is Co(II) > Zn(II) > Mn(II) > Cd(II). In oxalato complexes deaquation occurred in a single step in the sequence: Ni(II) > Fe(III) > Cu(II). For the malonato and succinato series a single step deaquation was noticed for Fe(III) and Cu(II) complexes. For oxalato, malonato and succinato complexes, the decomposition peak temperatures for reactions of the type $H_2[ML_2] \rightarrow MCO_3$, follow the order: Zn(II) > Ni(II) > Cd(II) > Mn(II) > Co(II), Ni(II) > Co(II) > Zn(II) > Cu(II) and Mn(II) ~ Co(II) > Ni(II) > Fe(II), respectively. Decomposition peak temperatures for reactions of the type $H_2[ML_2] \rightarrow MCO_3$ with the same central metal ion with different ligands follow the order: suc > ox > mal. The deaquation and decomposition of the complexes, $(NH_4)_3[Fe(ox)_3]$, $(NH_4)_2[Cu(suc)_2]$ and $(NH_4)_2[Zn(suc)_2]$ occurred in a single step and their pyrolysed product was the metal carbonate and the complex $(NH_4)_2[Fe(ox)_2] \cdot 2H_2O$; the pysolysis proceeded in a single step.

Activation energies (E_a^*) for the deaquation, deammoniation and decomposition processes were computed from TG curves by the Horowitz and Metzger method [2], and from DTA curves by using the Borchardt and Daniel equation [3], considering the order of reaction to be unity, their values are given in Tables 2–4, respectively. In most of the cases the values were more or less similar except for decomposition of $(NH_4)_3[Fe(ox)_3]$ and $H_2[Co(ox)_2]$ and for the dehydration of $(NH_4)_2[Cu(mal)_2] \cdot 2H_2O$. For these complexes the Coats and Redfern equation [4] was applied to evaluate their activation energies (E_a^*) but the values found were very low. In the deaquation and deammoniation processes the activation energies (E_a*) from TG curves for oxalato, malonato and succinato complexes follow the trend Co(II) > Mn(II) > Zn(II) > Cd(II), Ni(II) > Zn(II) > Fe(II) > Cu(II) > Co(II) and Mn(II) > Ni(II) > Co(II) > Fe(II), respectively. In the single-step deaquation process for oxalato complexes, the activation energy (E_a^*) follows the sequence Cu(II) > Ni(II) > Fe(III). Activation energy (E_a*) for the process, $H_2[ML_2] \rightarrow MCO_3$ for oxalato, malonato and succinato series are in the following order: Zn(II) > Cd(II) > Ni(II) > Co(II) > Mn(II), Ni(II) > Co(II) > Zn(II) > Fe(II) (obtained after reduction of Fe(III) complex) and Ni(II) > Co(II) > Fe(II) > Mn(II), respectively. The activation energy (E_a*) for the decomposition of, $(NH_4)_3[Fe(ox)_3] \rightarrow FeCO_3$ and $(NH_4)_2[Zn(suc)_2] \rightarrow ZnCO_3$ are 264.2 kJ mol^{-1} and 322.3 kJ mol^{-1}, respectively.

Enthalpy changes (ΔH) for the deaquation and deammoniation steps for oxalato, malonato and succinato complexes are in the order: Mn(II) > Cd(II) > Co(II) > Zn(II), Fe(II) > Co(II) > Ni(II) > Cu(II) > Mn(II) > Zn(II) > Cd(II) and Mn(II) > Ni(II) > Co(II) > Cd(II) > Fe(II), respec-

---

* For malonato complexes.

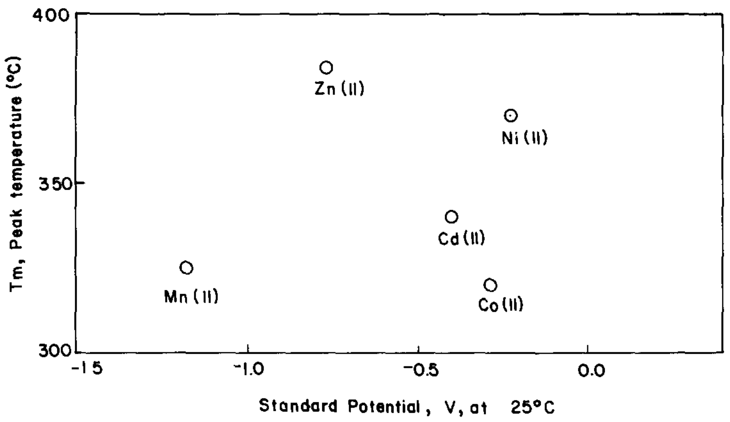

Fig. 4. Plots of decomposition peak temperature (T_m, °C) for $H_2[M(ox)_2] \rightarrow MCO_3$ vs. standard potential (V) of the central metal ion at 25°C.

tively. For the single-step deaquation process of oxalato complexes, the enthalpy changes (ΔH) and entropy changes (ΔS) are in the order Ni(II) > Cu(II) > Fe(III).

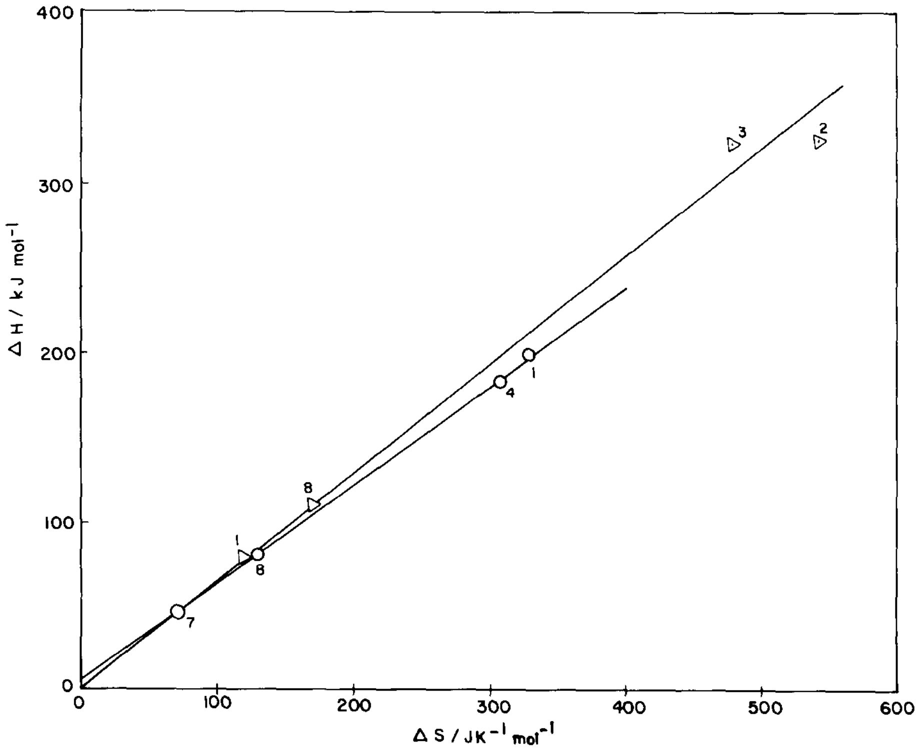

Fig. 5. Plots of ΔH vs. ΔS for the thermal decomposition, $H_2[ML_2] \rightarrow MCO_3$. (⊙——⊙) Oxalato complexes, 1 = Mn(II), 4 = Co(II), 7 = Zn(II), 8 = Cd(II). (△——△) Malonato complexes, 1 = Mn(II), 2 = Fe(II), 3 = Fe(III), 8 = Cd(II).

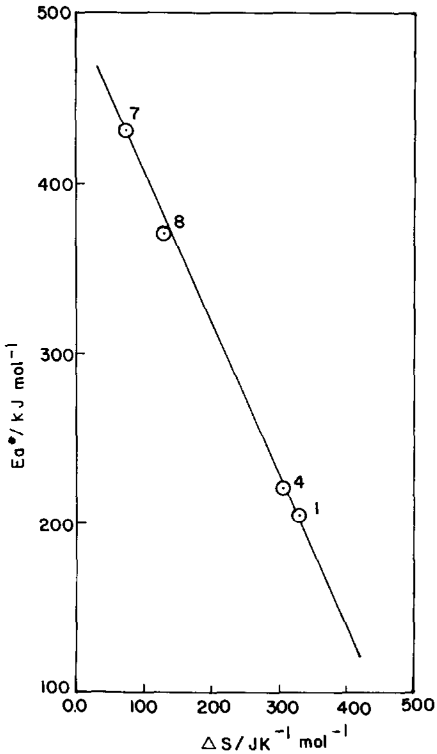

Fig. 6. Plots of E_a^* vs. ΔS for the thermal decomposition, $H_2[M(ox)_2] \rightarrow MCO_3$. 1 = Mn(II), 4 = Co(II), 7 = Zn(II) and 8 = Cd(II).

For malonato and succinato complexes, the deaquation occurred in a single step for Fe(III) and Cu(II) and their corresponding enthalpy changes (ΔH) are 109.8 kJ mol^{-1} and 124.4 kJ mol^{-1}, respectively.

The enthalpy changes (ΔH) for the process $H_2[ML_2] \rightarrow MCO_3$ for oxalato, malonato and succinato complexes follow the order: Mn(II) > Co(II) > Cd(II) > Zn(II), Ni(II) > Co(II) > Fe(II) (obtained after reduction of Fe(III) complex) > Cd(II) and Ni(II) > Co(II) > Fe(II) > Mn(II), respectively.

The entropy changes (ΔS) for the dequation and deammoniation processes of oxalato, malonato and succinato complexes follow the trends: Cd(II) > Mn(II) > Co(II) > Zn(II), Fe(II) > Co(II) > Cu(II) > Ni(II) > Zn(II) and Mn(II) > Co(II) > Ni(II) > Fe(II), respectively. The entropy changes (ΔS) for the process $H_2[M(ox)_2] \rightarrow MCO_3$ follow the same sequence as the enthalpy changes. For the decomposition of $H_2[Co(mal)_2] \rightarrow CoCO_3$ and $H_2[Fe(suc)_2] \rightarrow FeCO_3$ the values are 346.9 and 545.6 J K^{-1} mol^{-1}, respectively.

DTA peak temperatures (T_m) of oxalato complexes for the process $H_2[ML_2] \rightarrow MCO_3$ were plotted against the standard potential of the central metal ion (Fig. 4) *. It was noticed from these plots that the thermal stabilities of the complexes decrease approximately with the increase of the tendency of the central metal ion to capture the electron from the ligand ions. A similar trend is also followed by malonato and succinato complexes. An attempt has been made to correlate the thermal parameters, like enthalpy change (ΔH), with the entropy change (ΔS) and a linear correlation has been found by plotting ΔH vs. ΔS as shown in Fig. 5. The entropy change (ΔS) values were calculated [6] by the relation $\Delta S = \Delta H / T_m$. Figure 6 shows that a linear relationship is obtained by plotting E_a^* vs. ΔS. Thus a system having higher entropy change (ΔS) requires less activation energy (E_a^*) for decomposition. Similar observations were noticed for the dehydration and decomposition processes.

ACKNOWLEDGEMENTS

The authors are grateful to the Indian Association for the Cultivation of Science, Calcutta 32 for recording TG and DTA curves and to the Government of Manipur, Manipur (India) for the financial help under FIP Scheme to HLS.

REFERENCES

1 K. Nagase, Bull. Chem. Soc. Jpn., 45 (1972) 2166.
2 H.H. Horowitz and G. Metzger, Anal. Chem., 35 (1963) 1464.
3 H.J. Borchardt and F. Daniels, J. Am. Chem. Soc., 79 (1957) 41.
4 A.W. Coats and J.P. Redfern, Nature (London), 201 (1964) 68.
5 W.M. Latimer, The Oxidation State of the Elements and Their Potentials in Aqueous Solutions, Prentice-Hall, New York, 1952.
6 R. Roy, M. Chaudhury, S.K. Mandal and K. Nag, J. Chem. Soc., Dalton Trans., (1984) 1981.

---

* These potentials [5] were considered to measure the tendency of the central metal ions to capture electrons from the ligand ions forming an oxalato complex, since the D_q value of H_2O was approximately equal to that of $C_2O_4^{2-}$ ions.